Published in final edited form as:

Neuroimage. 2007 April 1; 35(2): 904–915. doi:10.1016/j.neuroimage.2006.12.022.

Circuitry underlying temporally extended spatial working memory

Charles F. Geier[*], **Krista E. Garver**, and **Beatriz Luna**

Laboratory of Neurocognitive Development, Department of Psychology, and the Center for the Neural Basis of Cognition University of Pittsburgh, Pittsburgh, PA, USA

Abstract

Extended maintenance delays decrease the accuracy of information stored in spatial working memory. In order to elucidate the network underlying sustained spatial working memory, 16 subjects were scanned using fast event-related fMRI as they performed an oculomotor delayed response task containing trials with “short” (2.5 s) or “long” (10 s) delay periods. Multiple cortical and subcortical regions were common to both delay trial types indicating core task regions. Three patterns of activity were found in a subset of core regions that reflect underlying processes: maintenance-related (e.g., left FEF, right supramarginal gyrus (SMG)), response planning-related (e.g., right FEF, SEF), and motor response-related (e.g., lateral cerebellum (declive)) activation. Several regions were more active during long than short delay trials, including multiple sites in DLPFC (BA 9, 46), indicating a circuitry dynamically recruited to support sustained working memory. Our results suggest that specialized brain processes support extended periods of working memory.

Keywords

fMRI; Oculomotor; Working memory; Maintenance; Cognition; DLPFC; FEF

Introduction

Visual spatial working memory (VSWM) refers to the cognitive ability to hold “on-line” information about stimuli that are no longer present in the external environment but are key to adaptive behavior (Baddeley, 1983, 1986; Baddeley et al., 1975; Fuster, 1997). VSWM bridges retrospective sensory and prospective motor processing (e.g., Curtis et al., 2004; Curtis, 2006) and underlies a wide range of complex, higher-order behaviors including spatial reasoning and problem solving (e.g., Newman et al., 2003).

It has been well established in humans and non-human primates that a widely-distributed brain circuitry supports VSWM. Single-unit studies in monkeys have identified distributed

[*]Corresponding author. University of Pittsburgh, 3501 Forbes Ave., Oxford Bldg, Room 738, Pittsburgh, PA 15213, USA. Fax: +1 412 246 6161. geiercf@upmc.edu (C.F. Geier).

Appendix A. Supplementary data: Supplementary data associated with this article can be found, in the online version, at doi:10.1016/j.neuroimage.2006.12.022.

populations of neurons with delay-contingent firing patterns that provide a neuronal mechanism for sustaining mnemonic information across a delay period. Such neurons have been identified in a number of cortical and sub-cortical regions, including prefrontal cortex (Funahashi et al., 1989, 1991, 1993, 1997), frontal eye field (FEF) (Funahashi et al., 1989), supplementary eye field (SEF) (Hanes et al., 1995), inferior parietal lobule (Colby et al., 1996; Gnadt and Andersen, 1988), caudate nucleus (Hikosaka et al., 1989a,b), thalamus (Wyder et al., 2004), and superior colliculus (Munoz and Wurtz, 1995; Basso and Wurtz, 1998). Delay-contingent reductions in firing patterns have also been observed in substantia nigra pars reticulata (SNpr) (Hikosaka and Wurtz, 1983). In humans, numerous neuroimaging studies collectively implicate recruitment of a widely distributed system supporting working memory, including dorsolateral prefrontal cortex (DLPFC), FEF, SEF, intraparietal sulcus (IPS), cingulate cortex, basal ganglia, and lateral cerebellum (e.g., Sweeney et al., 1995, 1996; McCarthy et al., 1996; Courtney et al., 1997, 1998; Smith and Jonides, 1998; Ungerleider et al., 1998; LaBar et al., 1999; Luna et al., 1999; Cabeza and Nyberg, 2000; Hartley and Speer, 2000; Postle et al., 2000a,b; Rowe et al., 2000; Berman and Colby, 2002; Leung et al., 2002; Manoach et al., 2003; Wager and Smith, 2003; Brown et al., 2004a,b; Curtis et al., 2004, 2005; Passingham and Sakai, 2004; Curtis and D'Esposito, 2006; Keedy et al., 2006; Klingberg, 2006; Ricciardi et al., 2006; Ranganath, 2006; Scherf et al., 2006).

The distributed network engaged to support performance of a VSWM task codes for multiple underlying cognitive processes. VSWM tasks typically consist of a fixed sequence of events: the initial presentation of a stimulus, a delay interval when the stimulus is not seen, and a cued execution epoch when a memory-guided response is executed. Different cognitive processes are emphasized during each epoch, including encoding (initial mapping of a characteristic of some stimulus into an internal representation), maintenance (retention of that representation across a delay), manipulation (engaging in an additional cognitive process during the delay period), response planning (using the maintained representation to guide purposeful action), and execution (generating a response).

The mechanisms underlying maintenance, in particular, have been of great interest in the literature. Most maintenance studies have examined the effects of increased memory load and/or manipulation demands during the delay period on various brain regions (e.g., Cohen et al., 1997; Rypma et al., 1999a,b; Jha and McCarthy, 2000; Leung et al., 2004; D'Esposito et al., 1999). A few studies have indicated increased activation in widespread frontal regions, such as left caudal inferior frontal gyrus and superior frontal gyrus, as memory load increases (e.g., Rypma et al., 1999a,b), and a primary role for DLPFC in the manipulation of information (e.g., D'Esposito et al., 1999). A more recent report provides evidence that prefrontal cortex plays less of a role in the storage of information than does a domain-specific network in posterior cortex (Postle, 2006). Together, these studies suggest a specific network supporting working memory *capacity*. However, we still have a limited understanding of the mechanisms that sustain information over time.

We have previously demonstrated that increases in the duration of the delay period can undermine the fidelity of maintained representations—longer delay periods in the oculomotor delayed response (ODR) task lead to decreased latency, implying ongoing

response preparation, and decreased accuracy of the saccadic response, indicating loss of signal (Luna et al., 2004). We do not yet, however, have a good understanding of the underlying network supporting temporally-extended delay periods. Our intent in the current study was to take a novel approach to understanding maintenance by characterizing the mechanisms that support spatial working memory throughout different lengths of working memory delays.

Two hypothetical network configurations may underlie extended maintenance. First, there may be a static, fixed network of regions recruited throughout a delay period, regardless of its duration. Extended delays would thus simply entail temporally-sustained activity in these areas. A second possibility is that a core network of regions *necessary* to perform the task is recruited early and additional regions that function to facilitate or enhance maintenance (e.g., by filtering out distractors, updating rule information, or 'refreshing' the maintained mnemonic information) are dynamically recruited later as duration demands increase.

We examine these two possible network configurations in the context of an oculomotor delayed response (ODR) task comprised of two trial types, each with different lengths of delay periods. The ODR task was developed for use in monkey electrophysiology studies (Hikosaka and Wurtz, 1983) and is particularly well-suited to investigate extended maintenance for a number of reasons. First, in the present design, encoding and motor response demands (the location of a briefly appearing flash and a saccade to the remembered location, respectively) are equivalent across short and long-delay trial types. This restricts subjects from adopting different encoding strategies based on advanced knowledge of the delay length of the upcoming trial. Second, the type and amount of information that is required to be maintained are also equivalent across delay trial types. Third, there are no manipulation demands in this task, minimizing potential misinterpretations of maintenance versus manipulation-related activity, particularly in prefrontal circuitry (e.g., Rowe et al., 2000). Only the length of time that the subject must hold the location information online is varied. Finally, given the relatively widespread use of ODR tasks in single-unit studies, implementation of this task with human subjects allows us to draw a link between the human and non-human primate literatures investigating the brain basis of VSWM.

In terms of the brain regions supporting VSWM trials with different delay durations, we hypothesized that a core set of regions, including the FEF, SEF, DLPFC, posterior parietal cortex, anterior cingulate, caudate, and the lateral cerebellum (e.g., Sweeney et al., 1995, 1996; Courtney et al., 1998; LaBar et al., 1999; Luna et al., 1999; Cabeza and Nyberg, 2000; Postle et al., 2000a,b; Rowe et al., 2000; Wager and Smith, 2003; Brown et al., 2004b; Curtis et al., 2004; Passingham and Sakai, 2004), would be recruited during each mnemonic trial type. We also hypothesized that there would be an additional subset of regions recruited to support the demands of extended maintenance, such as updating rule representation (e.g., DLPFC) over the longer delays.

A second level of analysis was possible based on our straightforward comparisons of the networks supporting short versus long delay trials. By comparing the patterns in the time courses from commonly recruited brain regions, we are able to gain additional insight on the functional contributions of these areas. We predicted that two basic patterns would be

observable in the time courses. First, regions involved in sustaining a memory trace across the duration of the delay period (similar to activity in some neurons with delay-contingent activity) were predicted to show early involvement during both delay trial types and prolonged activity on long-delay trials (see Fig. 1A), with no increases in magnitude (Boynton et al., 1996). Second, since subjects did not know if the delay on any given trial would be short or long (see Materials and methods), we predicted that time courses from regions associated with response preparation/execution (i.e., planning to initiate a saccade toward the remembered location of the stimulus) would show a single peak on short trials, but a biphasic response on long-delay trials (see Fig. 1B). That is, during long-delay trials, these regions should exhibit increased activity prior to when a motor response would be required on a short-delay trial, decreased activity when a motor response is not cued, then a second peak of activity towards the end of the longer delay when a response would actually be required.

Materials and methods

Subjects

Eighteen healthy adult subjects were recruited for this study. Imaging data from two subjects were excluded from analyses due to excessive (greater than 1/3 voxel) head motion in the scanner. The remaining 16 subjects (ages 18–30 years; 9 males) were right handed, had far visual acuity of at least 20/40 (corrected or uncorrected), and medical histories that revealed no neurological disease, brain injury, or major psychiatric illness in the subject or first degree relative. Written consent and experimental procedures for this study complied with the Code of Ethics of the World Medical Association (1964 Declaration of Helsinki) and the Institutional Review Board at the University of Pittsburgh. Subjects were paid for their participation in the study.

Oculomotor delayed response (ODR) task

Our task consisted of spatial working memory (a.k.a. oculomotor delayed response) trials and visually guided saccade (VGS) trials with jittered inter-trial fixation periods (see Fig. 2). In spatial working memory trials, (Fig. 2A), subjects were instructed to fixate a central yellow crosshair for 2425 ms. A brief (75 ms) stimulus randomly appeared at one of four possible locations on the horizontal meridian, at ±4° or ±8° of visual angle. Stimulus eccentricity was counterbalanced across visual hemi-fields. Subjects were explicitly instructed not to look at the stimulus when it appeared but to remember its location in space. A delay period followed presentation of the stimulus that lasted either 2.5 or 10 s (referred to as “short-delay” and “long-delay” trials, respectively). Importantly, subjects were instructed to maintain fixation during the delay as spatial working memory for locations has been shown to be disrupted by eye movement control (Postle et al., 2006). The fixation cross disappeared after the delay, which cued subjects to look toward the remembered location of the target. Subjects did not know the delay length of any given trial as these were randomly chosen. For the VGS trials (Fig. 2B), subjects first fixated a green cross for 1250 ms. A stimulus appeared (1250 ms) at one of four possible locations on the horizontal meridian, at ±4, 8° visual angle. Subjects were instructed to look at the peripheral target when it appeared. VGS trials were analyzed to assure that expected oculomotor regions were

engaged during the task, but were not considered in any additional statistical analyses. During fixation periods (Fig. 2C; presented between trials), subjects maintained fixation on a central white crosshair for jittered intervals of either 5, 7.5, 10, or 12.5 s, with the selection of each inter-trial fixation period duration determined using a decaying exponential function (Dale and Buckner, 1997; Dale, 1999). Twenty long-delay trials, 20 short-delay trials, and 20 VGS trials were presented in random order in each run; two runs were presented per experimental session.

Eye tracking

Each subject completed behavioral training on the ODR task in our laboratory no more than 1 week prior to being scanned. In the MR scanning environment, eye movements were obtained with a long-range optics eye-tracking system (Model 504LRO; Applied Science Laboratories, Bedford, MA, USA) that recorded eye position by pupil-corneal reflection obtained by a mirror mounted on the head coil. Simultaneous on-line video monitoring was used to assess task compliance. At the beginning of each eye-tracking session, a nine-point calibration procedure was performed. Fourteen subjects viewed experimental stimuli presented using Macromedia (Adobe) FLASH software while four subjects viewed the identical stimuli presented using E-Prime (Psychology Software Tools, Pittsburgh, PA). All stimuli were front-projected onto a flat screen positioned on a standard head coil. Recorded eye tracking data were viewed and scored off-line using a combination of ILAB software (Gitelman, 2002) and in-house scoring programs written in MATLAB (MathWorks, Inc.) running on a Dell Dimension 8300 PC. Due to limitations in the original set-up of the eye tracking system, we were able to obtain usable data for only seven subjects.

fMRI acquisition and preprocessing

Imaging data were collected using a 3.0 Tesla Signa whole-body MR scanner (General Electric Medical Systems, Milwaukee, WI). A gradient-echo echo-planar imaging sequence sensitive to blood-oxygen-dependent (BOLD) contrast (T2*) was performed (Kwong et al., 1992; Ogawa et al., 1992). The acquisition parameters were: TR=2.5 s; TE = 25 ms; flip angle = 90°; single shot; full k-space; 64×64 acquisition matrix with FOV = 20×20 cm. Twenty-three 5-mm-thick axial slices with a 1 mm gap were collected, aligned to the base of the genu and splenium of the corpus callosum, generating 3.125×3.125×5 mm voxels, which covered the entire cortex and most of the cerebellum. A three-dimensional volume spoiled gradient-echo (SPGR) pulse sequence with 124 slices (1.5 mm slice thickness) was used to acquire the structural images in the axial plane.

FIASCO software (Functional Imaging Analysis Software— Computational Olio) (Eddy et al., 1996) was used to pre-process the raw data. Images were corrected for three-dimensional head motion by aligning each volume in the time series to the volume obtained in the middle of the acquisition. Images were submitted to linear, temporal detrending by calculating an unbiased estimate of the slope and subtracting it out of each pixel's time series. Each subject's images were smoothed with a 5.6 mm full-width at half maximum (FWHM) filter, which given the original voxel size was optimal for maximally improving the signal-to-noise ratio while minimally reducing resolution, and shifted 5 s, which adjusts for the peak activation of the BOLD response function (Cohen et al., 1997).

fMRI data analyses

Individual subjects—Three-dimensional datasets were created from the two-dimensional preprocessed image files using AFNI (Analysis of Functional Neuro-Images) (Cox, 1996). Next, to convert from arbitrary image intensity units to percent signal change, we divided the time series of each voxel by its mean intensity. AFNI was then used to obtain event-related activation data via multiple regression to overlay on co-planar anatomic images (Cox, 1996). Detailed methods for this procedure have been described fully elsewhere (Ward, 1998). Briefly, for each subject, the BOLD response to each trial type (i.e., ODR "long" trials, ODR "short" trials, and visually guided saccade trials—not analyzed here) was estimated by coding a different regressor (i.e., delta function) for each of the 15 time points (i.e., image acquisitions) immediately following each trial onset. This procedure produced one time course estimate over 15 time points per voxel, per trial type. The selected time lag (15 TRs) was sufficiently long to capture the rise and fall of the hemodynamic response for each trial type. We did not assume a response shape in our time course estimation. Note that the estimated BOLD response from ODR trials encompassed presentation of the cue, delay period, and the motor response. Individual ODR trial components were not modeled in this study. Jittered inter-trial fixation periods (see the Oculomotor delayed response (ODR) task section) ensured that there were a sufficient number of independent linear equations to estimate the BOLD responses separately. Each individual map was then spatially normalized into Talairach space (Talairach and Tournoux, 1988) using anatomical markers and re-sampled into 1 mm isotropic voxels.

Group analyses—In this study, we aimed to 1) identify brain regions supporting trials with different maintenance durations, and 2) characterize the function of 'core' brain regions by examining the hemodynamic time courses in these areas during short and long-delay trials. To address our first aim, we conducted voxel-wise analysis of variance (ANOVA) on the short-delay trial estimated BOLD response values from each subject with time (TR 1 through 15) as a fixed factor and subjects (16) as a random factor. This resulted in a main effect of time map for the short-delay trial condition identifying regions that were significantly ($p< 0.005$) active across time. Since subjects did not know at the start of each trial which delay would be forthcoming, encoding and early maintenance requirements were equivalent across trials. Therefore, the task-related areas involved in short-delay trials would also be recruited during long-delay trials. Regions exhibiting a main effect of time for the short trial condition were thus considered in our experiment to be reflective of a core spatial working memory network.

We then repeated the above procedure using the long-delay trial estimated BOLD response values. Regions identified in long-delay trials that were absent in the short-delay trials may represent areas that assist maintenance regions in sustaining the fidelity of a representation across prolonged delay periods. The main effect of time maps for both short- and long-delay trials were corrected for multiple comparisons using False Discovery Rate (FDR). Threshold was set for these images at $p<0.01$.

Clusters identified in the main effect of time maps were simultaneously compared to an anatomically-defined ROI database (27 regions of interest across 2 hemispheres) drawn in

AFNI in order to assess which brain regions were recruited during each trial type. Details of the construction of this ROI mask are provided elsewhere (Scherf et al., 2006). A region was considered "common" to short and long-delay trials if it contained clusters of significantly (p<0.01, corrected) activated voxels from both the short and long-delay trial main effect of time maps.

To address our second aim of characterizing response mechanisms of core regions supporting short- and long-delay trials, we first used the clusters from the short-trial main effect of time map as a functional mask and extracted the average estimated BOLD time course from these voxels across subjects for both the short- and long-delay trials. We then performed repeated measures ANOVA with condition (short and long-delay trials), time (TR 1 through 15), and subjects (N=16) as factors on these time courses. We did this in order to make direct statistical comparisons of the responses in the same voxels across delay trial types.

To investigate the hypothesis that additional regions may come on-line during longer delay periods to assist or facilitate aspects of extended maintenance, we identified clusters observed exclusively in the long-delay trial main effect of time map. It is possible that these same regions were also participating during short-delay trials but simply did not reach our selected level of significance and thus were not detected in the short main effect of time map. To account for this possibility, we used clusters exclusively identified in the long-delay trial main effect of time map as functional masks and extracted the estimated mean BOLD time courses from the corresponding voxels across subjects for both short-and long-delay trials. These extracted time courses were then subjected to further statistical analyses. First, repeated-measures ANOVA was conducted to examine whether the short-delay trial time course from a particular region had a significant main effect of time. If significant (p<0.05), another repeated-measures ANOVA was conducted to examine the relationship between short and long-delay trial time courses across time. If not, then the region was considered to be active only in the long delay trials.

Results

Scanner eye tracking

Video monitoring of subjects' eyes during scanning provided online visual evidence of task compliance for all 16 participants. Due to technical limitations at time of acquisition, however, eye tracking data from only 7 out of 16 subjects were able to be scored for overall percent correct (i.e., proportion of correctly performed ODR trials) and initial saccade latency. Noise artifact precluded analyses of saccade accuracy to the 0.5° to 1° of visual angle of spatial resolution needed to assess differences due to the delay period. Overall percent correct across both delay trials was extremely high among these 7 subjects (M=99.1±1.4%). Across all trials, only one error was observed: one subject incorrectly broke fixation and made a saccade towards the peripheral cue. This error occurred during a long-delay trial. Removal of this subject from analyses did not change our overall results. As expected due to longer preparation times, latencies for the initial saccade made following long delays (M=484.43±55.04 ms) were significantly shorter than for short delays (M=510.59±10.59 ms), $t(4)=5.587$, p<0.005.

ROI analysis

Common clusters—As expected, short- and long-delay trials were supported by largely overlapping networks (Fig. 3). Clusters were identified in several commonly reported ROIs (see Materials and methods), including bilateral FEF, right SEF, left DLPFC (BA 10/46) (Talairach coordinates: −44, 46, 18), left IPS, and the right caudate. We also observed activation bilaterally in the anterior inferior parietal lobule, adjacent to the postcentral sulcus, anterior and distinct from the supramarginal gyrus. In 11 out of 16 subjects, a common cluster in the left declive (cerebellum) was also identified. Additional regions were recruited as well during both delay trial types, including bilateral superior temporal gyrus, left parahippocampal gyrus, right middle cingulate, and left medial dorsal thalamus. A complete list of common regions, including Talairach coordinates and *F*-statistic for the peak voxel in each cluster, can be found in Table 1.

Long-delay trial clusters—Clusters identified in a more caudal location in the left DLPFC (BA 46) (Talairach coordinates: −43, 39, 10), anterior cingulate, and bilateral regions in the lateral cerebellum (simple lobule) were found to be non-overlapping between the two main effect of time maps. In addition, multiple clusters at various sites in bilateral DLPFC (BA 9,10), bilateral pre-supplementary motor area (Pre-SMA), right middle cingulate, left middle temporal gyrus, and bilateral inferior frontal gyrus (BA 47) were also identified only in the long-delay trial main effect of time map at the significance level reported ($p<0.01$, corrected). A comprehensive list of these regions can be found in Table 2.

Time course analyses

Commonly recruited task regions—Three distinguishable patterns were observed in the BOLD time courses from a subset of the commonly recruited brain regions. Table 3 lists the region from which these time courses have been extracted as well as the Talairach coordinates of the peak voxel from each cluster.

Pattern 1: In left FEF, left middle temporal gyrus (BA 39), and right supramarginal gyrus (SMG), trials with short delays exhibited single-peaked (occurring between 12.5 s and 15 s post trial-onset), relatively broad, time courses. For long delay trials, the responses in these regions were roughly similar in magnitude but temporally extended (Fig. 4).

Repeated-measures ANOVA on the time courses for pattern 1 revealed the following effects: left FEF (trial type ($F(1,15)=5.826$, $p<0.05$); time ($F(14,210)=7.589$, $p<0.001$)); trial type by time interaction ($F(14,210)=3.201$, $p<0.001$)), left middle temporal gyrus (trial type = not significant; time ($F(14,210)=6.060$, $p<0.001$); trial type by time interaction ($F(14,210)=1.774$, $p<0.05$)), and right SMG (trial type ($F(1,15)=8.857$, $p<0.01$); time ($F(14,210)=3.419$, $p<0.001$); trial type by time interaction ($F(14,210)=2.768$, $p<0.001$)).

Pattern 2: A second pattern was observed in the right FEF, right SEF, left IPS, and right superior temporal gyrus. In these time courses, a single peak is observed in short trials, occurring between 10 and 12.5 s post trial onset (Fig. 5). In long-delay time courses from these regions, a bi-phasic response is observed. Initially, the long-trial time course rises simultaneously with the short-trial time course, until approximately 7.5–10 s post trial onset.

This initial peak is followed by a decrease in percent signal change, and then by a second peak. This second peak occurs in each of these regions 20 s after the start of the trial and is roughly similar in magnitude (within approximately 0.10% MR signal change) to the short trial peak.

Repeated-measures ANOVA on the time courses for pattern 2 revealed the following effects: right FEF (trial type = not significant; time ($F(14,210) = 7.307$, $p< 0.001$); trial type by time interaction ($F(14,210) = 6.509$, $p< 0.001$)), right SEF (trial type = not significant; time ($F(14,210) = 6.987$, $p< 0.001$); trial type by time interaction ($F(14,210) = 6.589$, $p< 0.005$)), right superior temporal gyrus (trial = not significant; time ($F(14,210) = 8.328$, $p< 0.001$); trial type by time interaction ($F(14,210) = 4.346$, $p< 0.001$)), and left IPS (trial = not significant; time ($F(14,210) = 5.321$, $p< 0.001$); trial type by time interaction ($F(14,210) = 7.159$, $p<0.001$)).

Pattern 3: A third pattern was observed in left lingual gyrus (BA 17/18) and in the left declive of the cerebellum (Fig. 6). The HDR in these regions consisted of a single, relatively broad peak in both short and long trials. Short-delay trials peaked earlier (15 s) than long-delay trials (between 20 and 22.5 s). Relative to the short and long trial peaks observed in pattern 2, short and long trial peaks in pattern 3 both occurred later in time.

Repeated-measures ANOVA on the time courses for pattern 3 revealed the following effects: left lingual gyrus (trial type=not significant; time ($F(14,210)=5.790$, $p<0.001$); trial type by time interaction ($F(14,210)=3.919$, $p<0.001$)) and left declive (trial type=not significant; time ($F(14,140)=10.893$, $p<0.001$); trial type by time interaction ($F(14,140)=2.906$, $p<0.001$)).

Long delay trial clusters—Repeated-measures ANOVA (factors: time, subjects) on the mean time courses for short-delay trials extracted from long-delay trial cluster masks revealed no significant main effect of time for right inferior frontal gyrus, left inferior frontal gyrus, right middle frontal gyrus, and left lateral cerebellum (simple lobule). A significant main effect of time was observed in right medial frontal gyrus ($F(14,210)=2.869$, $p<0.001$), left DLPFC ($F(14,210)=2.061$, $p<0.05$), right superior frontal gyrus $F(14,210)=2.147$, $p<0.05$), right Pre-SMA ($F(14,210) = 2.265$, $p < 0.001$), left Pre-SMA ($F(14,210)=3.265$, $p<0.001$), left anterior cingulate ($F(14,210) = 2.294$, $p<0.01$), left middle temporal gyrus ($F(14,210)=2.204$, $p<0.01$), right cuneus ($F(14,210)=2.654$, $p<0.001$), left precuneus ($F(14,210)=2.538$, $p<0.005$), and right lateral cerebellum (simple lobule) ($F(14,210)=2.468$, $p<0.005$).

Repeated-measures ANOVA (factors: trial type, time, subjects) was again conducted to explore the relationship between the short and long-trial time courses extracted from long main effect of time clusters. These analyses excluded those clusters that did not exhibit a significant time course in the short-delay trial (See Above). The following effects were observed: right medial frontal gyrus (trial type =not significant; time ($F(14,210)= 4.738$, $p<0.001$); trial type by time interaction=not significant), left DLPFC (trial type ($F(1,15)=7.393$, $p<0.05$); time ($F(14,210) = 3.691$, $p<0.001$); trial type by time interaction=not significant), right superior frontal gyrus (trial type=not significant; time

($F(14,210)=4.019$, $p<0.001$); trial type by time interaction=not significant), right pre-SMA time courses (trial type=not significant; time ($F(14,210)=6.273$, $p<0.001$); trial type by time interaction = not significant); left pre-SMA (trial type=not significant; time ($F(14,210)=5.507$, $p<0.001$); trial type by time interaction=not significant), left anterior cingulate (trial type=not significant; time ($F(14,210)=4.698$, $p<0.001$); trial type by time interaction=not significant), left middle temporal gyrus (trial type=not significant; time ($F(14,210)=4.625$, $p<0.001$); trial type by time interaction = not significant), right cuneus (trial type=not significant; time ($F(14,210)=5.856$, $p< 0.001$); trial type by time interaction ($F(14,210)=2.081$, $p<0.05$)), left cuneus (trial type=not significant; time ($F(14,210) =4.338$, $p< 0.001$); trial type by time interaction ($F(14,210)=1.934$, $p<0.05$)), right lateral cerebellum (simple lobule) (trial type=not significant time; time ($F(14,210) = 4.780$, $p<0.001$); trial type by time interaction ($F(14,210)=1.794$, $p<0.05$)).

Discussion

Visual spatial working memory allows for the internal, online maintenance of spatial information in the absence of externally driving sensory inputs (Baddeley, 1983, 1986; Baddeley et al., 1975; Fuster, 1997). Performance of VSWM tasks necessitates coordinated encoding, maintenance, manipulation (when necessary), response planning, and motor execution processes. In the ODR task used in the current study, where trial types were identical except for the duration of the delay period, maintenance processes were emphasized and explored. Specifically, we aimed to characterize the network(s) supporting working memory maintenance across extended relative to shorter delay periods.

Not surprisingly, based on the gross similarities between the two delay trials, our results indicated that largely overlapping distributed circuitries support both delay trial types. Clusters of significantly active voxels were found in regions frequently identified as contributing to VSWM tasks, including bilateral FEF, right SEF, bilateral anterior inferior parietal lobule, left IPS, right caudate, and left DLPFC (BA 10/46) (e.g., Sweeney et al., 1995, 1996; McCarthy et al., 1996; Courtney et al., 1997, 1998; Smith and Jonides, 1998; Ungerleider et al., 1998; LaBar et al., 1999; Luna et al., 1999; Cabeza and Nyberg, 2000; Hartley and Speer, 2000; Postle et al., 2000a, b; Rowe et al., 2000; Berman and Colby, 2002; Leung et al., 2002; Manoach et al., 2003; Wager and Smith, 2003; Brown et al., 2004a,b; Curtis et al., 2004, 2005; Passingham and Sakai, 2004; Schluppeck et al., 2005, 2006; Curtis and D'Esposito, 2006; Keedy et al., 2006; Klingberg, 2006; Ricciardi et al., 2006; Ranganath, 2006; Postle, 2006; Scherf et al., 2006). The fact that these regions, along with others listed in Table 1, were recruited despite differences in the maintenance duration requirements suggests that they support ‘core’ components of visual spatial working memory task performance such as encoding, response planning, fundamental aspects of maintenance, and/or the motor response.

Importantly, there were also several differences in the underlying networks supporting different delay lengths. The most striking differences in the long-delay circuitry was the recruitment of several sites in the DLPFC, including clusters in right BA 9, bilateral BA 10, and right BA 46 (a distinct and more ventral location relative to the commonly recruited DLPFC (BA 46/10) cluster). The recruitment of additional prefrontal areas as delay length

increases is similar to the findings of Rypma et al. (1999a, b) demonstrating load-dependent engagement of various regions in prefrontal cortex during a verbal working memory task. Our results suggest that the brain responds to increases in delay length in a VSWM task similarly to increases in load, despite an equivalent number of items being remembered. In addition to these prefrontal areas, several other regions, such as right anterior cingulate, bilateral lateral cerebellum (simple lobule), and bilateral pre-supplementary motor areas were also recruited more in long-delay trials.

The more ventral cluster observed in the left DLPFC (BA 46) may reflect processes engaged in order to protect the fidelity of the maintained spatial information during longer delays. One proposed function of prefrontal cortex is to protect memories from distraction, perhaps by recurrent interaction of excitatory and inhibitory circuits in prefrontal cortex or between PFC and posterior association areas (Compte et al., 2000; Sakai et al., 2002). Our results are similar to Sakai et al. (2002), who identified a region in BA 46 where there was reactivation of maintained verbal working memory. The lateral cerebellum and its connections to the dentate nucleus of the cerebellum form a loop through thalamus to provide outputs to BA 46 (Middleton and Strick, 1994, 2001). The bilateral clusters observed in the lateral cerebellum (simple lobule) may assist DLPFC in processes needed to sustain or reactivate working memory information over extended delay periods.

The anterior cingulate gyrus has been associated with detection of conflicts in information processing (e.g., Botvinick et al., 1999; Carter et al., 1999). During the longer delays, error detection processes mediated by the anterior cingulate may come online because of an incongruence with response preparation processes activated early during the delay period and the lack of a cue to respond (i.e., the central cross hair does not disappear at 2.5 s during long delay trials).

In summary, our findings related to the network configurations of short and long-delay trials confirm the results of previous investigations implicating a widely distributed circuitry underlying VSWM tasks. We propose that the common areas observed in different delay trials reflect a core set of regions necessary for task performance. Importantly, we add to the literature by providing evidence that there are dynamically recruited regions that contribute as well; specific brain regions either come online (e.g., right inferior frontal gyrus) or increase their relative participation (e.g., left DLPFC) when extended periods of maintenance are required. Although regions significantly activated during the long-delay trials like the anterior cingulate may reflect processes related to conflicts in information processing (a consequence of the paradigm used), regions such as the DLPFC and the lateral cerebellum (simple lobule) may function to facilitate the maintenance of a memory trace over extended delay durations, perhaps by mediating processes to filter out distractors or to re-update the remembered spatial location of the stimulus.

Discerning functional roles based on differences in the time courses

By characterizing differences in short- and long-delay hemodynamic time courses from core task regions, we were able to gain additional insight on the functional contributions of these regions. Three distinct patterns were identified based on these comparisons.

First, in left FEF, left middle temporal gyrus (BA 39), and supramarginal gyrus, trials with short delays exhibited positive, single-peaked, relatively broad time courses. On long-delay trials, these regions exhibited time courses which were similar in magnitude but extended in time. This pattern of activity, which we term “maintenance-related”, was predicted for regions that function to sustain a mnemonic representation for the duration of the delay period.

Brain imaging findings in humans suggest that the middle temporal gyrus (MTG) plays a key role in the storage of declarative rule knowledge (see Bunge, 2004). Thus, one explanation of MTG engagement throughout the delay periods of the different trial types is that the subjects were actively maintaining the task rules (e.g., “Remember the location of the flashed stimulus”). A sustained representation of task rules would be essential for successful behavioral performance.

The frontal eye field has been typically associated with response preparation, but is consistently detected in working memory neuroimaging studies (e.g., Gaymard et al., 1999; Postle et al., 2000a; Corbetta et al., 2002; Brown et al., 2004b; Curtis and D'Esposito, 2006; Postle, 2006). Our results involving *left* FEF suggest that there may be bilateral differences in the functional role of FEF: left FEF may participate in maintenance of the spatial location of a stimulus, while right FEF participates in response preparation and execution processing. An alternative explanation is that the left FEF may be involved in processes related to holding fixation on the central crosshair during the delay period (Petit et al., 1999), which could result in a time course pattern similar to our maintenance-related pattern.

Areas near the supramarginal gyrus (SMG) have been found to be involved in the generation of saccades and in shifts of attention (Perry and Zeki, 2000). Specifically, it has been suggested that the SMG is recruited when a decision must be made regarding the future execution of a saccade, keeping the saccade system “on alert” as to the possibility of a response (Perry and Zeki, 2000). In our task, subjects were unaware of when a saccade would be required. This aspect of the task may have required a persistent state of preparedness supported by processing in the SMG.

Collectively, this first pattern of activity occurs in regions typically associated with sustaining information across a delay or maintaining a state of readiness or alertness. Interestingly, these regions are similar to areas where populations of neurons with delay-contingent activity have been identified in non-human primates (Funahashi et al., 1989; Colby et al., 1996; Gnadt and Andersen, 1988), suggesting a comparable underlying mechanism used to maintain information for prolonged periods.

A second pattern, observed in clusters identified in the right FEF, right SEF, right superior temporal gyrus, and left IPS, was characterized by a single peak in short trials and a biphasic response in long-delay time courses that did not return to baseline in between peaks. One explanation for this pattern is that they indicate involvement in response preparation and/or execution. Indeed, the frontal eye field and supplementary eye field have been found to play crucial roles in the planning of voluntary eye movement responses based on single-cell and neuroimaging studies (e.g., Chen and Wise, 1995; Curtis, 2006; Funahashi et al., 1991,

1989; Hanes et al., 1995; Schall, 1991; Mann et al., 1988; Olson and Gettner, 1995; Schlag and Schlag-Rey, 1987; Tehovnik et al., 2000). Based on the patterns in the time courses and consideration of the timing of the components of the ODR trials, our results provide additional evidence that these regions play a role in response preparation. The first peak in the biphasic response in long-delay trials is very similar to the early rise of the short trial time course, indicating similar early processes during both delays. However, the long-delay time courses also exhibited a second peak. From the subjects' naïve perspective on the forthcoming delay length, preparing to make a saccade early in the delay period, regardless of whether or not they would actually have to execute it, may be an appropriate strategy for optimal task performance. On trials that turn out to have long delays, this initial preparatory activity may be reduced and then ramped up again towards the end of the longer delay. Thus, in the long-delay time courses, the early peak may reflect a ‘false start’ in response planning whereas the second peak reflects preparatory processes for the forthcoming, cued saccadic response.

The lack of a complete return to baseline in pattern 2 time courses could indicate that these regions are also involved in sustained delay period activity. Recently, Schluppeck et al. (2006) characterized sustained bilateral activation in IPS during a memory guided saccade task at different delay intervals. The IPS activation observed in our study (Talairach coordinates: −17, −76, 47) is anatomically close to the “IPS1” and “IPS2” regions previously reported (Schluppeck et al., 2005, 2006). Further, qualitative similarities can be observed with their time courses from IPS2 at delays of 3 and 10.5 s (similar to the delay period durations used in the present study). Pattern 2 may thus reflect transient activity related to the initial visual target, sustained activity during the delay period, and a transient response to the saccade at the end of the delay period (Schluppeck et al., 2006).

Taken together, our results indicate that pattern 2 regions may be involved in both response preparation and maintenance processes. The addition of a third, longer delay period (∼20 s) in a future study would instantiate a third possible time to respond and thus could help dissociate response preparation related processing from sustained activity plus two transients, as noted in IPS by Schluppeck and colleagues.

A third, unpredicted pattern was observed in a cluster in left declive and left lingual gyrus (BA 17/18). The hemodynamic response function from this region consisted of a single, relatively broad peak in short trials and a similar, but time-shifted response in long trials. Importantly, the peaks during short trials in this region occurred later in the time course than the peaks in response planning regions. Although this pattern may reflect a time-lagged hemodynamic response from these areas, another possibility is that these patterns reflect underlying processes that are more closely tied to preparing for the actual motor response (i.e., response execution) or, alternatively, processes which occur after the initial saccade to the target location has been made (e.g., in the assessment of the accuracy of the memory guided saccade). Future studies will be needed in order to test these explanations. The declive may support memory guided saccade accuracy via connections to nuclei in the vermis (known to support the accuracy of saccadic eye movements) and would be recruited close to the response itself (Leigh and Zee, 1999). Activity near the lingual gyrus, a visual

association area, may provide sensorimotor input involved in the assessment of memory-guided saccade accuracy that is also tied to directing the actual motor response.

Conclusions

Working memory is known to operate over time periods ranging from a few to tens of seconds (Baddeley, 1983, 1986; Baddeley et al., 1975; Fuster, 1997), but the neural processes underlying extended maintenance are relatively unknown. Our work, aimed at a more complete characterization of maintenance processes, indicates that a core circuitry supports working memory across time, regardless of the length of the delay period. Our time course analyses allowed us to partially differentiate the functional roles of a number of these regions, including middle temporal, inferior parietal, and left FEF involvement in sustained maintenance, premotor (right FEF, SEF) recruitment in response planning, and cerebellar and visual association regions' involvement in processes more closely related to the actual motor response. Importantly, our results are consistent with the notion that spatial selective attention and motor preparatory processes are fundamental to spatial working memory function (e.g., Postle, 2006). We also found evidence that areas beyond the core working memory regions were recruited or exhibited increased involvement when extended periods of maintenance were required, including several sites in DLPFC (BA 9, 10, 46), right anterior cingulate, and regions in the lateral cerebellum (simple lobule). Taken together, these results suggest that working memory circuitry is influenced by the extent of the delay and that there may be specific processes which support the ability to retain information online for prolonged periods.

Supplementary Material

Refer to Web version on PubMed Central for supplementary material.

Acknowledgments

The authors give thanks to Melanie Wilds-Liebmann, Enami Yasui, and Matthew Costello for valuable assistance in data collection, as well as to Miya Asato, K. Suzanne Scherf, and Katerina Velanova for helpful discussions on the manuscript. The authors also give special thanks to all participants of this study. Supported by MH01727 and MH067924.

References

Baddeley, A. Working Memory. Oxford Univ. Press; New York: 1986.

Baddeley AD. Working memory. Philos Trans R Soc London, Ser B Biol Sci. 1983; B302:311–324.

Baddeley, AD.; Grant, S.; Wight, E.; Thomson, N. Attention and Performance V. Erlbaum; 1975. Imagery and visual working memory; p. 205-217.

Basso MA, Wurtz RH. Modulation of neuronal activity in superior colliculus by changes in target probability. J Neurosci. 1998; 18(18):7519–7534. [PubMed: 9736670]

Berman RA, Colby CL. Spatial working memory in human extrastriate cortex. Physiol Behav. 2002; 77(4–5):621–627. [PubMed: 12527009]

Botvinick M, Nystrom LE, Fissell K, Carter CS, Cohen JD. Conflict monitoring versus selection-for-action in anterior cingulated cortex. Nature. 1999; 402:179–181. [PubMed: 10647008]

Boynton GM, Engel SA, Glover GH, Heeger DJ. Linear systems analysis of functional magnetic resonance imaging in human V1. J Neurosci. 1996; 16:4207–4221. [PubMed: 8753882]

Brown JW, Bullock D, Grossberg S. How laminar frontal cortex and basal ganglia circuits interact to control planned and reactive saccades. Neural Netw. 2004a; 17(4):471–510. [PubMed: 15109680]

Brown MR, DeSouza JF, Goltz HC, Ford K, Menon RS, Goodale MA, Everling S. Comparison of memory- and visually guided saccades using event-related fMRI. J Neurophysiol. 2004b; 91(2): 873–889. [PubMed: 14523078]

Bunge SA. How we use rules to select actions: a review of evidence from cognitive neuroscience. Cogn Affect Behav Neurosci. 2004; 4(4):564–579. [PubMed: 15849898]

Cabeza R, Nyberg L. Imaging cognition II: An empirical review of 275 PET and fMRI studies. J Cogn Neurosci. 2000; 12:1–47. [PubMed: 10769304]

Carter CS, Botvinick MM, Cohen JD. The contribution of the anterior cingulate cortex to executive processes in cognition. Rev Neurosci. 1999; 10:49–57. [PubMed: 10356991]

Chen LL, Wise SP. Neuronal activity in the supplementary eye field during acquisition of conditional oculomotor associations. J Neurophysiol. 1995; 73:1101–1121. [PubMed: 7608758]

Cohen JD, Perlstein WM, Braver TS, Nystrom LE, Noll DC, Jonides J, et al. Temporal dynamics of brain activation during a working memory task. Nature. 1997; 386:608. [PubMed: 9121584]

Colby CL, Duhamel JR, Goldberg ME. Visual, presaccadic, and cognitive activation of single neurons in monkey lateral intraparietal area. J Neurophysiol. 1996; 76:2841–2852. [PubMed: 8930237]

Compte A, Brunel N, Goldman-Rakic PS, Wang XJ. Synaptic mechanisms and network dynamics underlying spatial working memory in a cortical network model. Cereb Cortex. 2000; 10:910–923. [PubMed: 10982751]

Corbetta M, Kincade JM, Shulman GL. Neural systems for visual orienting and their relationships to spatial working memory. J Cogn Neurosci. 2002; 14(3):508–523. [PubMed: 11970810]

Courtney SM, Ungerleider LG, Kell K, Haxby JV. Transient and sustained activity in a distributed neural system for human working memory. Nature. 1997; 386:608–611. [PubMed: 9121584]

Courtney SM, Petit L, Maisog JM, Ungerleider LG, Haxby JV. An area specialized for spatial working memory in human frontal cortex. Science. 1998; 279:1347–1351. [PubMed: 9478894]

Cox RW. AFNI: Software for analysis and visualization of functional magnetic resonance neuroimages. Comput Biomed Res. 1996; 29:162–173. [PubMed: 8812068]

Curtis CE. Prefrontal and parietal contributions to spatial working memory. Neuroscience. 2006; 139:173–180. [PubMed: 16326021]

Curtis CE, D'Esposito M. Selection and maintenance of saccade goals in the human frontal eye fields. J Neurophysiol. 2006; 95(6):3923–3927. [PubMed: 16467423]

Curtis CE, Rao VY, D'Esposito M. Maintenance of spatial and motor codes during oculomotor delayed response tasks. J Neurosci Off J Soc Neurosci. 2004; 24:3944–3952.

Curtis CE, Sun FT, Miller LM, D'Esposito M. Coherence between fMRI time-series distinguishes two spatial working memory networks. NeuroImage. 2005; 26(1):177–183. [PubMed: 15862217]

Dale AM. Optimal experimental design for event-related fMRI. Hum Brain Mapp. 1999; 8:109–114. [PubMed: 10524601]

Dale AM, Buckner RL. Selective averaging of rapidly presented individual trials using fMRI. Hum Brain Mapp. 1997; 5:329–340. [PubMed: 20408237]

D'Esposito M, Postle BR, Ballard D, Lease J. Maintenance versus manipulation of information held in working memory: an event-related fMRI study. Brain Cogn. 1999; 41:66–86. [PubMed: 10536086]

Eddy, WF.; Fitzgerald, M.; Genovese, CR.; Mockus, A.; Noll, DC. Functional image analysis software —Computational olio. In: Prat, A., editor. Proceedings in Computational Statistics. Physica-Verlag; Heidelberg: 1996. p. 39-49.

Funahashi S, Bruce CJ, Goldman-Rakic PS. Mnemonic coding of visual space in the monkey's dorsolateral prefrontal cortex. J Neurophysiol. 1989; 61:331–349. [PubMed: 2918358]

Funahashi S, Bruce CJ, Goldman-Rakic PS. Neuronal activity related to saccadic eye movements in the monkey's dorsolateral prefrontal cortex. J Neurophysiol. 1991; 65:1464–1483. [PubMed: 1875255]

Funahashi S, Inoue M, Kubota K. Delay-related activity in the primate prefrontal cortex during sequential reaching tasks with delay. Neurosci Res. 1993; 18:171–175. [PubMed: 8127467]

Funahashi S, Inoue M, Kubota K. Delay-period activity in the primate prefrontal cortex encoding multiple spatial positions and their order of presentation. Behav Brain Res. 1997; 84:203–223. [PubMed: 9079786]

Fuster, JM. The Prefrontal Cortex. 3rd. Raven Press; New York: 1997.

Gaymard B, Ploner CJ, Rivaud-Pechoux S, Pierrot-Deseilligny C. The frontal eye field is involved in spatial short-term memory but not in reflexive saccadic inhibition. Exp Brain Res. 1999; 129(2): 288–301. [PubMed: 10591903]

Gitelman DR. ILAB: a program for postexperimental eye movement analysis. Behav Res Methods, Instrum Comput :J Psychon Soc Inc. 2002; 34:605–612.

Gnadt JW, Andersen RA. Memory related motor planning activity in posterior parietal cortex of macaque. Exp Brain Res. 1988; 70:216–220. [PubMed: 3402565]

Hanes DP, Thompson KG, Schall JD. Relationship of presaccadic activity in frontal eye field and supplementary eye field to saccade initiation in macaque: Poisson spike train analysis. Exp Brain Res. 1995; 103:85–96. [PubMed: 7615040]

Hartley AA, Speer NK. Locating and fractionating working memory using functional neuroimaging: storage, maintenance, and executive functions. Microsc Res Tech. 2000; 51(1):45–53. [PubMed: 11002352]

Hikosaka O, Wurtz RH. Visual and oculomotor functions of monkey substantia nigra pars reticulata. III. Memory-contingent visual and saccade responses. J Neurophysiol. 1983; 49:1268–1284. [PubMed: 6864250]

Hikosaka O, Sakamoto M, Usui S. Functional properties of monkey caudate neurons. I. Activities related to saccadic eye movement. J Neurophysiol. 1989a; 61:780–798. [PubMed: 2723720]

Hikosaka O, Sakamoto M, Usui S. Functional properties of monkey caudate neurons III. Activities related to expectation of target and reward. J Neurophysiol. 1989b; 61:814–832. [PubMed: 2723722]

Jha AP, McCarthy G. The influence of memory load upon delay-interval activity in a working-memory task: an event-related functional MRI study. J Cogn Neurosci. 2000; 12:90–105. [PubMed: 11506650]

Keedy SK, Ebens CL, Keshavan MS, Sweeney JA. Functional magnetic resonance imaging studies of eye movements in first episode schizophrenia: smooth pursuit, visually guided saccades, and the oculomotor delayed response task. Psychiatry Res. 2006; 146(3):199–211. [PubMed: 16571373]

Klingberg T. Development of a superior frontal–intraparietal network for visuo-spatial working memory. Neuropsychologia. 2006; 44(11):2171–2177. [PubMed: 16405923]

Kwong KK, Belliveau JW, Chesler DA, Goldberg IE, Weisskoff RM, Poncelet BP, et al. Dynamic magnetic resonance imaging of human brain activity during primary sensory stimulation. Proc Natl Acad Sci U S A. 1992; 89:5675–5679. [PubMed: 1608978]

LaBar KS, Gitelman DR, Parrish TB, Mesulam M. Neuroanatomic overlap of working memory and spatial attention networks: a functional MRI comparison within subjects. NeuroImage. 1999; 10:695–704. [PubMed: 10600415]

Leigh, RJ.; Zee, DS. The Neurology of Eye Movements. 3rd. Oxford Univ. Press; New York: 1999.

Leung HC, Gore JC, Goldman-Rakic PS. Sustained mnemonic response in the human middle frontal gyrus during on-line storage of spatial memoranda. J Cogn Neurosci. 2002; 14:659–671. [PubMed: 12126506]

Leung HC, Seelig D, Gore JC. The effect of memory load on cortical activity in the spatial working memory circuit. Cogn Affect Behav Neurosci. 2004; 4(4):553–563. [PubMed: 15849897]

Luna B, Minshew NJ, Keshavan MS, Merriam EP, Eddy WE, Thulborn KR, et al. Spatial working memory improves from late childhood to adulthood: Eye movement and fMRI studies. 1999:1142.

Luna B, Garver KE, Urban TA, Lazar NA, Sweeney JA. Maturation of cognitive processes from late childhood to adulthood. Child Dev. 2004; 75:1357–1372. [PubMed: 15369519]

Mann SE, Thau R, Schiller PH. Conditional task-related responses in monkey dorsomedial frontal cortex. Exp Brain Res. 1988; 69:460–468. [PubMed: 3371430]

Manoach DS, Greve DN, Lindgren KA, Dale AM. Identifying regional activity associated with temporally separated components of working memory using event-related functional MRI. NeuroImage. 2003; 20:1670–1684. [PubMed: 14642477]

McCarthy G, Puce A, Constable RT, Krystal JH, Gore JC, Goldman-Rakic P. Activation of human prefrontal cortex during spatial and nonspatial working memory tasks measured by functional MRI. Cereb Cortex. 1996; 6:600–611. [PubMed: 8670685]

Middleton FA, Strick PL. Anatomical evidence for cerebellar and basal ganglia involvement in higher cognitive function. Science. 1994; 266:458–461. [PubMed: 7939688]

Middleton FA, Strick PL. Cerebellar projections to the prefrontal cortex of the primate. J Neurosci. 2001; 21(2):700–712. [PubMed: 11160449]

Munoz DP, Wurtz RH. Saccade-related activity in monkey superior colliculus. I. Characteristics of burst and buildup cells. J Neurophysiol. 1995; 73(6):2313–2333. [PubMed: 7666141]

Newman SD, Carpenter PA, Varma S, Just MA. Frontal and parietal participation in problem solving in the Tower of London: fMRI and computational modeling of planning and high-level perception. Neuropsychologia. 2003; 41:1668–1682. [PubMed: 12887991]

Ogawa S, Tank DW, Menon R, Ellermann JM, Kim SG, Merkle H, et al. Intrinsic signal changes accompanying sensory stimulation: functional brain mapping with magnetic resonance imaging. Proc Natl Acad Sci U S A. 1992; 89:5951–5955. [PubMed: 1631079]

Olson CR, Gettner SN. Object-centered direction selectivity in the macaque supplementary eye field. Science. 1995; 269:985–988. [PubMed: 7638625]

Passingham D, Sakai K. The prefrontal cortex and working memory: physiology and brain imaging. Curr Opin Neurobiol. 2004; 14:163–168. [PubMed: 15082320]

Perry RJ, Zeki S. The neurology of saccades and covert shifts in spatial attention: an event-related fMRI study. Brain. 2000; 123(11):2273–2288. [PubMed: 11050027]

Petit L, Dubois S, Tzourio N, Dejardin S, Crivello F, Michel C, Etard O, Denise P, Roucoux A, Mazoyer B. PET study of the human foveal fixation system. Hum Brain Mapp. 1999; 8(1):28–43. [PubMed: 10432180]

Postle BR. Distraction-spanning sustained activity during delayed recognition of locations. NeuroImage. 2006; 30:950–962. [PubMed: 16413797]

Postle BR, Berger JS, Taich AM, D'Esposito M. Activity in human frontal cortex associated with spatial working memory and saccadic behavior. J Cogn Neurosci. 2000a; 12:2–14. [PubMed: 11506643]

Postle BR, Zarahn E, D'Esposito M. Using event-related fMRI to assess delay-period activity during performance of spatial and nonspatial working memory tasks. Brain Res Protoc. 2000b; 5:57–66.

Postle BR, Idzikowski C, Sala SD, Logie RH, Baddeley AD. The selective disruption of spatial working memory by eye movements. Q J Exp Psychol (Colchester). 2006; 59(1):100–120.

Ranganath C. Working memory for visual objects: complimentary roles of inferior temporal, medial temporal, and prefrontal cortex. Neuroscience. 2006; 139(1):277–289. [PubMed: 16343785]

Ricciardi E, Bonino D, Gentili C, Sani L, Pietrini P, Vecchi T. Neural correlates of spatial working memory in humans: a functional magnetic resonance imaging study comparing visual and tactile processes. Neuroscience. 2006; 139(1):339–349. [PubMed: 16324793]

Rowe JB, Toni I, Josephs O, Frackowiak RSJ, Passingham RE. The prefrontal cortex: response selection or maintenance within working memory? Science. 2000; 288:1656–1660. [PubMed: 10834847]

Rypma B, d'Amato T, D'Esposito M. The roles of prefrontal brain regions in components of working memory: effects of memory load and individual differences. Proc Natl Acad Sci U S A. 1999a; 96:6558–6563. [PubMed: 10339627]

Rypma B, Prabhakaran V, Desmond JE, Glover GH, Gabrieli JDE. Load-dependent roles of frontal brain regions in the maintenance of working memory. NeuroImage. 1999b; 9:216–226. [PubMed: 9927550]

Sakai K, Rowe JB, Passingham RE. Active maintenance in prefrontal area 46 creates distractor-resistant memory. Nat Neurosci. 2002; 5:479–584. [PubMed: 11953754]

Schall JD. Neuronal activity related to visually guided saccadic eye movements in the supplementary motor area of Rhesus monkeys. J Neurophysiol. 1991; 66:530–558. [PubMed: 1774585]

Scherf KS, Sweeney JA, Luna B. Brain basis of developmental change in visuospatial working memory. J Cogn Neurosci. 2006; 18(7):1045–1058. [PubMed: 16839280]

Schlag J, Schlag-Rey M. Evidence for a supplementary eye field. J Neurophysiol. 1987; 57:179–200. [PubMed: 3559671]

Schluppeck D, Glimcher P, Heeger DJ. Topographic organization for delayed saccades in human posterior parietal cortex. J Neurophysiol. 2005; 94:1372–1384. [PubMed: 15817644]

Schluppeck D, Curtis CE, Glimcher PW, Heeger DJ. Sustained activity in topographic areas of human posterior parietal cortex during memory-guided saccades. J Neurosci. 2006; 26(19):5098–5108. [PubMed: 16687501]

Smith EE, Jonides J. Neuroimaging analyses of human working memory. Proc Natl Acad Sci U S A. 1998; 95(20):12061–12068. [PubMed: 9751790]

Sweeney JA, Mintun MA, Rosenberg DR, Luna B, Thulborn KR. PET and fMRI studies of spatial working memory. Am Coll Neuropsychopharmacol. 1995; 34:223.

Sweeney JA, Luna B, Berman RA, McCurtain BJ, Strojwas MH, Voyvodic JT, et al. fMRI studies of spatial working memory. Soc Neurosci. 1996; 22(664.6):1688.

Talairach, J.; Tournoux, P. Co-Planar Stereotaxic Atlas of the Human Brain. Thieme Medical Publishers; New York: 1988.

Tehovnik EJ, Sommer MA, Chou IH, Slocum WM, Schiller PH. Eye fields in the frontal lobes of primates. Brain Res Rev. 2000; 32:413–448. [PubMed: 10760550]

Ungerleider LG, Courtney SM, Haxby JV. A neural system for human visual working memory. Proc Natl Acad Sci U S A. 1998; 95(3):883–890. [PubMed: 9448255]

Wager TD, Smith EE. Neuroimaging studies of working memory: a meta-analysis. Cogn Affect Behav Neurosci. 2003; 3:255–274. [PubMed: 15040547]

Ward, BD. Deconvolution Analysis of fMRI Time Series Data Documentation for the AFNI Software Package. 1998. http://afni.nimh.nih.gov/afni/docps/3dDeconvolve.ps

Wyder MT, Massoglia DP, Stanford TR. Contextual modulation of central thalamic delay-period activity: representation of visual and saccadic goals. J Neurophysiol. 2004; 91(6):2628–2648. [PubMed: 14762161]

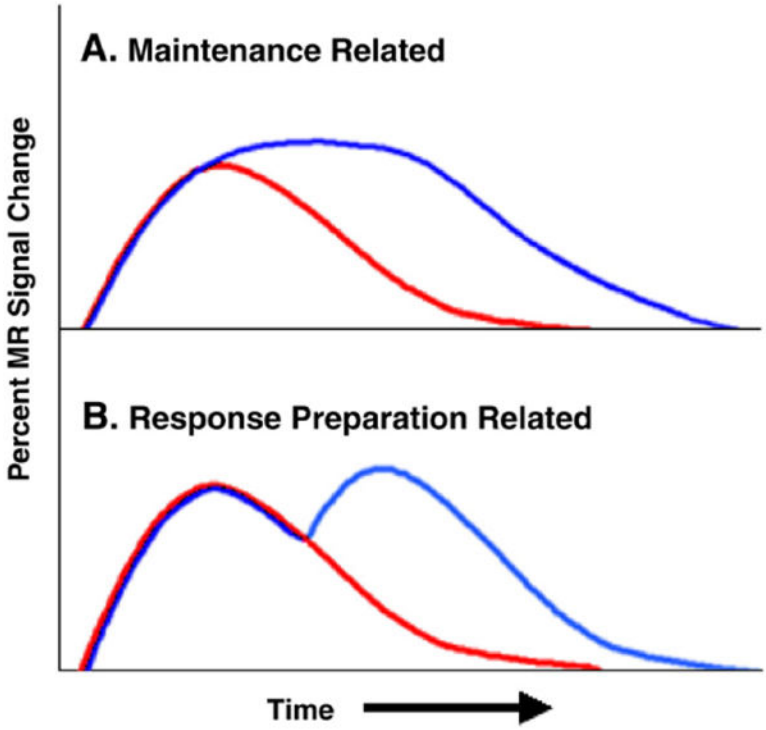

Fig. 1.

Expected hemodynamic time courses for (A) maintenance-related and (B) response preparation-related regions across short- (red trace) and long- (blue trace) delay trial types.

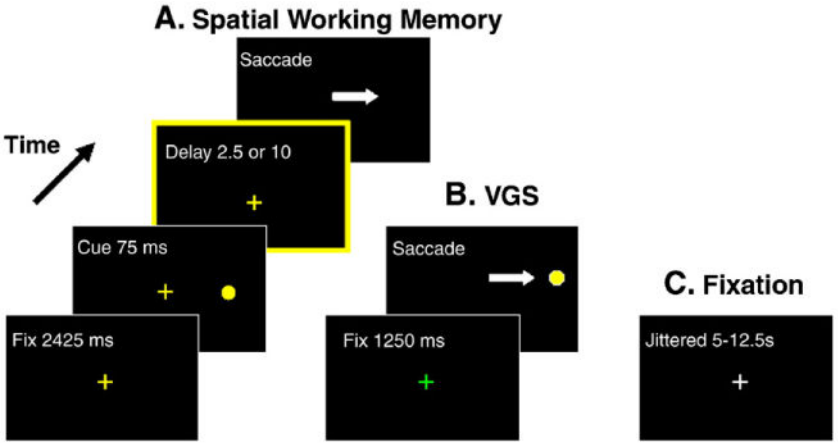

Fig. 2.

The oculomotor delayed response (ODR) task consisted of memory-guided saccade (MGS) trials (A) and visually-guided saccade trials (B), with a jittered fixation baseline (C). Arrows indicate the correct location of saccade on MGS and VGS trials. The colors of the fixation cross prior to the onset of each trial distinguished MGS and VGS.

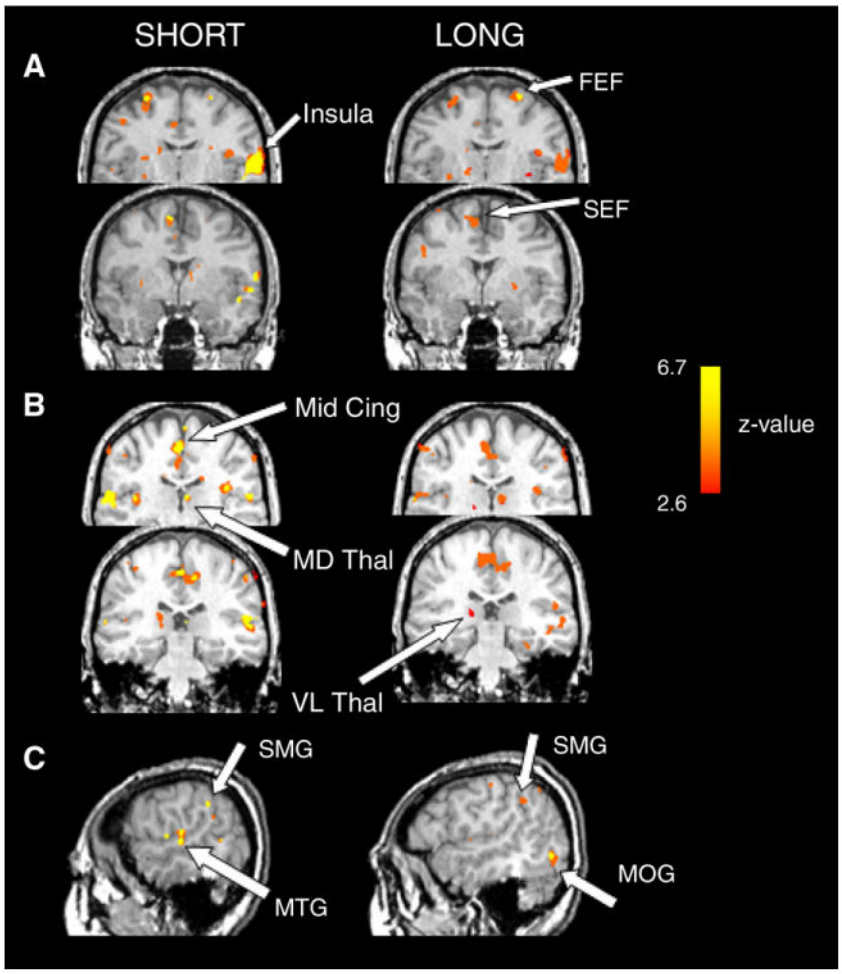

Fig. 3.

Examples of commonly recruited brain regions across short- and long-delay trial types. All images are thresholded at $p<0.01$, corrected. Radiological convention is used (e.g., right side of image=left hemisphere of the brain). Abbreviations: FEF=frontal eye field; SEF=supplementary eye field; Mid Cing=middle cingulate gyrus; MD Thal=medial dorsal nucleus of the thalamus; VLThal=ventral lateral nucleus of the thalamus; SMG=supramarginal gyrus; MTG=middle temporal gyrus; MOG=middle occipital gyrus.

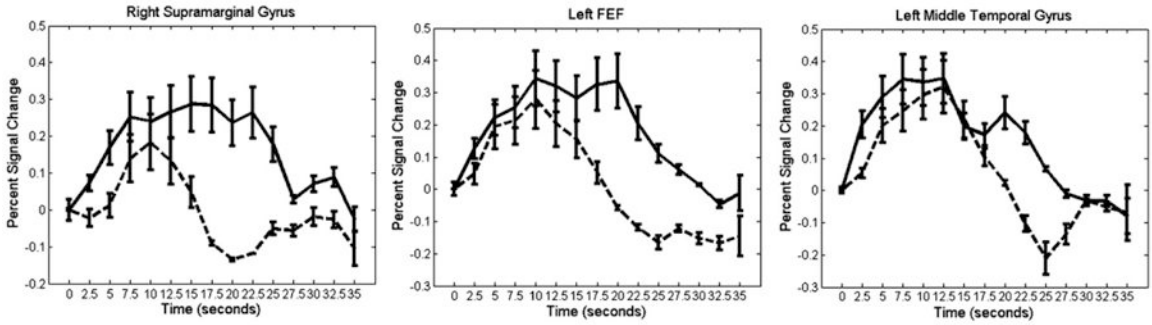

Fig. 4.

Brain regions exhibiting pattern 1 (“maintenance-related”) time courses. For each graph, the dashed line depicts the mean short-delay time courses and the solid line depicts the mean long-delay time course. Error bars represent the standard error of the mean at each time point.

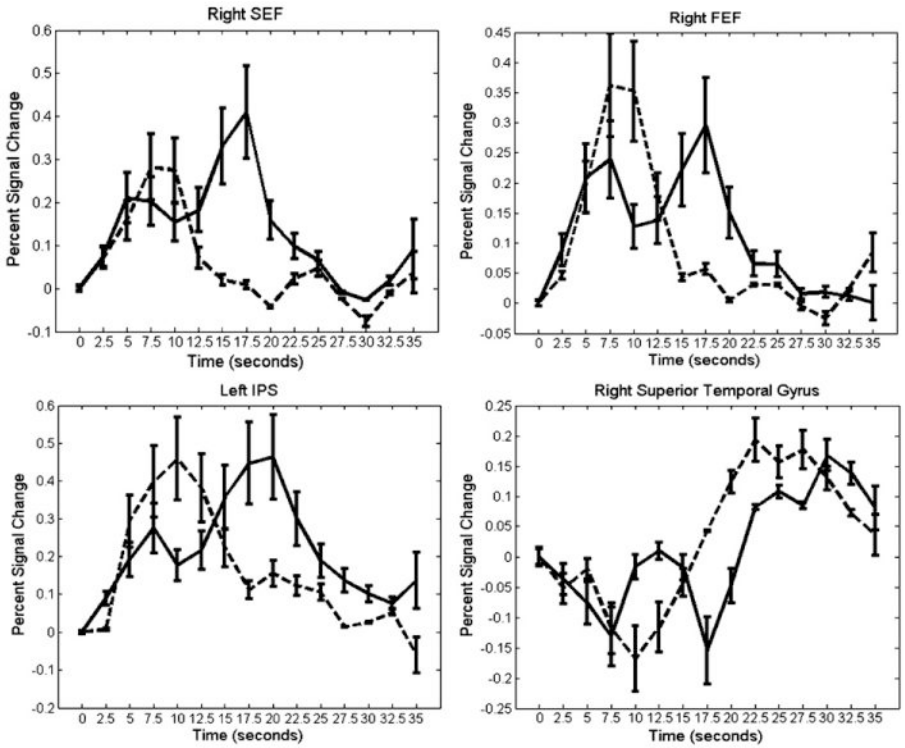

Fig. 5.

Brain regions exhibiting pattern 2 (“response preparation-related”) time courses. For each graph, the dashed line depicts the mean short-delay time courses and the solid line depicts the mean long-delay time course. Error bars represent the standard error of the mean at each time point.

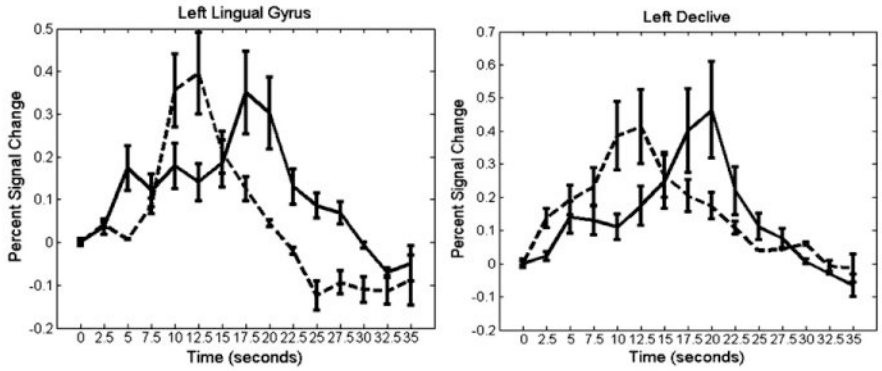

Fig. 6.

Brain regions exhibiting pattern 3 (“motor response-related”) time courses. For each graph, the dashed line depicts the mean short-delay time courses and the solid line depicts the mean long-delay time course. Error bars represent the standard error of the mean at each time point.

Table 1

Brain regions recruited during short- and long-delay trials

Talairach coordinates			Region	BA	Peak *F*
x	*y*	*z*			
			Frontal		
9	−1	56	Right SEF	6	5.64
−28	−12	63	Left FEF	6	5.03
24	−7	61	Right FEF	6	6.83
4	−19	49	Right middle cingulate	6,31	10.51
−44	46	18	Left DLPFC	10,46	4.21
			Parietal		
36	−37	58	Right anterior inferior parietal lobule	40	6.13
−40	−34	55	Left anterior inferior parietal lobule	40	5.82
50	−44	35	Right supramarginal gyrus	40	6.01
−17	−76	47	Left IPS	7	5.01
			Temporal		
40	−31	9	Right superior temporal gyrus	41	8.03
−60	−6	10	Left superior temporal gyrus	22	8.26
−54	−60	11	Left middle temporal gyrus	39	4.48
−29	−17	−11	Left parahippocampal gyrus	35	3.61
−32	21	−1	Left insula	13	4.78
36	−21	7	Right insula	13	6.8
			Occipital		
−8	−94	−9	Left lingual gyrus	17/18	4.91
49	−66	−5	Right middle occipital gyrus	37	3.92
			Sub-cortical		
−4	−24	9	Left MD thalamus	–	4.56
15	−11	1	Right thalamus, ventral lateral nucleus	–	4.49
16	−6	18	Right caudate body	–	4.14
−28	−12	−1	Left putamen	–	5.24
25	−7	12	Right putamen	–	4.67

Talairach coordinates			Region	BA	Peak *F*
x	*y*	*z*			
−31	−69	−26	Left declive	–	4.66

Table 2

Brain regions recruited during long-delay trials

Talairach coordinates			Region	BA	Peak *F*
x	*y*	*z*			
			Frontal		
38	26	−1	Right inferior frontal gyrus	47	4.69
−42	28	−5	Left inferior frontal gyrus	47	4.91
32	44	29	Right middle frontal gyrus	9	5.39
8	59	16	Right medial frontal gyrus	10	4.52
−43	39	10	Left DLPFC	46	4.31
7	48	47	Right superior frontal gyrus	8	4.43
6	11	59	Right pre-SMA	6	4.79
−1	21	49	Left pre-SMA	8	5.05
−3	45	1	Left anterior cingulate	32	5.89
2	13	44	Right cingulate gyrus	32	3.78
			Temporal		
−32	−58	29	Left middle temporal gyrus	39	6.01
			Occipital		
3	−83	22	Right cuneus	18	6.99
−2	−62	33	Left precuneus	17	4.44
			Sub-cortical		
33	−49	−38	Right lateral cerebellum (simple lobule)	–	4.74
−32	−55	−30	Left lateral cerebellum (simple lobule)	–	4.81

Table 3
Common regions used in time course pattern analysis

Talairach coordinates			Region	BA
x	*y*	*z*		
			Pattern 1	
−28	−12	63	Left FEF	6
−54	−60	11	Left middle temporal gyrus	39
50	−44	35	Right supramarginal gyrus	40
			Pattern 2	
24	−7	61	Right FEF	6
9	−1	56	Right SEF	6
40	−31	9	Right superior temporal gyrus	41
−17	−76	47	Left IPS	7
			Pattern 3	
−8	−94	−9	Left lingual gyrus	17/18
−31	−69	−26	Left declive	–